Nonlinear and stochastic dynamics in a forced vibro-impact energy harvester

Daniil Yurchenko*, Larissa Serdukova† and Rachel Kuske †
* *Department of Mechanical Engineering, Heriot-Watt, Edinburgh UK*
†*School of Mathematics, Georgia Tech, Atlanta, GA, USA*

Summary. Vibro-impact (VI) energy harvesting (EH) systems represent a class of highly nonlinear (non-smooth) systems with impact-type component interactions. A recently proposed VI-EH device, comprises a main mass, subjected to an external excitation, and a smaller mass within, traveling freely in a slot in between two dielectric elastomer (DE) membranes, deforming them at impact. As a highly flexible polymer with high dielectric permittivity and nonlinear responses properties, DE has desirable properties given its chemical composition, response to excitation, superior energy density and suitability for low frequency applications. In order to predict the specific performance of the VI-EH device, we develop a new (semi)-analytical approach for analysis of nonlinear stochastic dynamics in non-autonomous non-smooth impacting systems. This methodology relies on capturing the bifurcation structure and its influence on output energy, providing insight into the role of dynamics in energy harvesting efficiency and in the optimal design of the device. The analysis also reveals a generic mechanism and energy transfer phenomenon in nonlinear impacting systems.

Complex dynamics of the vibro-impact energy harvester (VI-EH)

The proposed VI-EH device is a vibro-impacting mechanical system, consisting of a cylinder of length s and mass M, an inner ball with mass m ($M \gg m$) moving within the cylinder between impacts with dielectric elastomer (DE) membranes at both ends of the cylinder. The system is inclined with an angle of β and forced with a harmonic excitation $F(\omega t + \phi)$ along the direction of its axis. We neglect friction between the ball and the cylinder, and track the relative position $Z = X - x$, for X the non-dimensionalized displacement of the cylinder center and x the location of the ball. The equation of motion and impact condition for the k^{th} impact at time $t = t_k$ are

$$\ddot{Z} = f(t) + \bar{g}, \quad f(t) = F(\omega t + \varphi), \qquad \dot{Z}_k^+ = -r\dot{Z}_k^-, \;\; Z_k = \pm\frac{d}{2}, \quad Z_k = Z(t_k). \tag{1}$$

Here $\bar{g} = -Mg \sin\beta/\|F\|$, where g is gravity, and $\|F\|$ the norm of F. The impact condition is applied on the bottom (top) ∂B (∂T) membrane of the VI-EH device at $(x - X) = \pm d/2$ for $d = \frac{s}{x_c}$, with $\dot{Z}^\pm$ the non-dimensionalised relative velocity of the ball before (-) (after (+)) impact and r the restitution coefficient. The parameter d captures the influence of length, amplitude of excitation, and frequency via the factor $x_c = \frac{\|\hat{F}\|\pi^2}{M\omega^2}$. Integrating (1) between impacts for $t \in (t_{k-1}, t_k)$ yields

$$\dot{Z}(t) = -r\dot{Z}_{k-1}^- + \bar{g}(t - t_{k-1}) + F_1(t) - F_1(t_{k-1}), \;\; F_1(t) = \int f(t)dt, \tag{2}$$

and integrating (2) we get the analogous equation for $Z(t)$. At the k^{th} impact, the maps for $\dot{Z}_k^-$ and Z_k^- are obtained by taking $t = t_k$ in (2) and the similar equation for Z, with $Z_k = \pm d/2$ at impact. Combining these maps we get all possible motions of the ball, $P_1 : \partial B \mapsto \partial T$, $P_2 : \partial T \mapsto \partial B$, $P_3 : \partial B \mapsto \partial B$, $P_4 : \partial T \mapsto \partial T$.

Using P_j together with the impact conditions and F periodic, we first study periodic motions of an inclined VI-EH, such as those shown in the phase planes of Fig. 1 (Left). The nonlinear analysis provides the bifurcation and stability conditions for different types of behavior within a non-dimensionalized framework, allowing us to capture the results in terms of dependence on parameters d, r, and β, and excitation, also considered in [1] for $\beta = 0$. For an incline $\beta \neq 0$, gravity naturally contributes to the asymmetric state and different nonlinear behaviors. We find transitions and stability for two families of periodic solutions. The first has a 1:1 ratio of impacts on ∂T to ∂B per excitation period, obtained by alternating P_1 and P_2. The analysis shows that these 1:1 behaviors are characterized by the triples $(\dot{Z}_k, \phi_k, \Delta t_k)$. Here ϕ_k is the phase difference between the impact and a trough (or peak) of F, and $\Delta t_k = t_{k+1} - t_k$. A second family has a 1:n ratio of impacts on ∂T and ∂B. These follow from grazing bifurcations and are composed of P_3, P_1, P_2. In Fig. 1 (Middle) we show these families in terms of $\dot{Z}_k$ from numerics for a range of d. Analytical solutions reproduce these branches in [2]. As shown in Fig. 1 (Left and Middle) for decreasing d, there are periodic doublings of the 1:1 family ($d > d_{\mathrm{graz}} \approx .2$, d_{graz} corresponding to a grazing bifurcation), until the grazing bifurcation leads to the 1:2 ratio of impacts ($d < .2$). Following an impact on δB, non-monotonic behavior of the relative velocity $\dot{Z}$ appears as a loop in the phase plane trajectory after $\dot{Z}$ crosses 0 on the trajectory away from $Z = \pm d/2$. For d_{graz} we have $\dot{Z}_{k+1} = Z_{k+1} = 0$, corresponding to a transition to P_3 before P_2, yielding a 1:2 solution.

Energy is harvested via impacts with the DE membranes, with $U_{\mathrm{imp}}^{(i)}$ the voltage at the i^{th} impact obtained from geometrical parameters of the membrane and $\dot{Z}_i$ [4]. The harvested voltage $U_{imp} - U_{in}$ is shown in Fig. 1 (Middle), for U_{in} a constant input voltage applied to the membranes, and d decreases with increasing amplitude of forcing $\|F\|$. Note that grazing bifurcations and 1:2 periodic solutions correspond to low velocity impacts, yielding an abrupt loss of average energy output per impact.

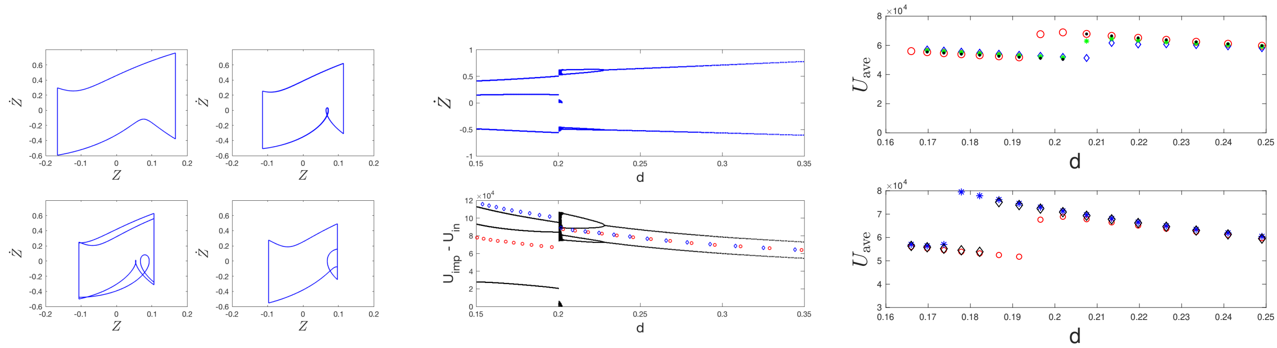

Figure 1: (Left). Limit cycles in the phase plane for Z,$\dot{Z}$ with different sequences of impacts in the VI-EH model (1) for decreasing d; all but lower right with 1:1 ratio per period of forcing, lower right is 2:1. Middle Upper: Impact velocity $\dot{Z}_k$ vs. d; Lower: Corresponding output voltage (black), red (blue) for average output per impact (unit time); Right: Average energy output per impact. Red circles for small constant β and no feedback; Upper: blue for larger β, symmetrically distributed, green and black for asymmetric distribution of β with small mean. Lower: blue and black for different levels of feedback.

Influence of randomness

The analytical results provided by the nonlinear maps reveal potential sensitivities to certain parameters for the different states, indicating conditions under which stochastic effects influence transitions. For example, the dependency of grazing bifurcations on ϕ_k suggests that stochastic fluctuations in the phase can benefit energy output by disrupting low velocity impacts. We derive stochastic nonlinear maps describing probabilistic transitions between states, thus capturing both detrimental and beneficial effects of random fluctuations on the energy output.

The stochastic variations of the maps P_j are derived from the physical model, depending on the stochastic source and transition of interest. Such variations were found in [3], which considered stochastic versions of the Nordmark map for compliant impacts near grazing. The phase plane analysis in [2] motivates a simple efficient formulation to study the behavior near the underlying period doubling bifurcations, based on considering separately the stochastic versions of P_1 and P_2 to capture the dilation of trajectories in $\dot{Z}_k$ on P_2. A similar dilation of ϕ_k on P_1 indicates a complementary approach, that capitalizes on the sensitivity to $\phi_k \ll 1$, as already suggested from the nonlinear expressions of $\sin \phi_k$ in the triple $(\dot{Z}_k, \phi_k, \Delta t_k)$ for the 1:1 families [2]. To capture the influence of parameter uncertainties, we break P_j into submaps, between key points corresponding to $\dot{Z} = 0$, $Z = \pm d/2$, and $\ddot{Z} = 0$, all important features in the approach to grazing shown in Fig 1 (Left).

We find that certain noise in ϕ, relaxing rapidly to fluctuations about its mean, yields an averaging effect that generates an effective reduction in the forcing amplitude. Then the attracting 1:1 periodic behavior is sustained over a larger range of d. Specifically, for smaller d, the 1:2 behavior is displaced, as is the corresponding lower average energy output per impact.

Fig. 1 (Right) shows the influence of other noise and asymmetries on U_{ave} vs. d. Certain random fluctuations in β advance d_{graz} to larger values, even counter-intuitively for asymmetric distributions of β with a small average $\overline{\beta} \ll 1$. If there is a non-negligible tail probability for $\beta = O(1)$ (green and black markers in Fig. 1 (Right upper)), the average energy output is closer to that obtained for random $\beta = O(1)$ (blue diamonds) than for smaller deterministic β (red circles), suggesting that even for short transient periods of $\beta = O(1)$, the system remains in the 1:2 behavior over a longer time period. Also, feedback of the capsule motion at a lagged time leads to an effective phase shift in the forcing, potentially avoiding repeated ∂B impacts for $\phi_k \ll 1$ (blue and black markers in Fig. 1 Right lower) and shifting reduced U_{ave} to smaller d. There are a number of ways to model this effect, including randomness to capture lack of precise feedback. The newly derived stochastic maps near the critical transitions related to 1:1 and 1:2 periodic solutions explain how noise influences transitions between different levels of energy output.

Conclusions

Semi-analytical nonlinear analyses of a novel model for vibro-impact energy harvesting (VI-EH) captures parametric and excitation dependencies of the output voltage. The results point to parameter ranges and scenarios where noise and asymmetries can be either detrimental or beneficial for the energy output. Via novel stochastic analyses and computations, we reveal the sensitivities of the system to random fluctuations and asymmetries. These indicate analysis-based design features for the VI-EH device.

References

[1] A. Luo, *Journal of Vibration and Acoustics*, 124, 420-426, (2002).

[2] L. Serdukova, R. Kuske, and D. Yurchenko, *Nonlinear Dynamics* (to appear). https://doi.org/10.1007/s11071-019-05289-8.

[3] D.J.W. Simpson and R. Kuske, *J. Vibration and Control,* 24, 407-426, 2016.

[4] D. Yurchenko, D. V. Val, Z. H. Lai, G. Gu, and G. Thomson, *Smart Mater. Struct.,* 26, 105001, 2017.